

The quasiparticle spectral function in doped graphene

E. H. Hwang and S. Das Sarma

Condensed Matter Theory Center, Department of Physics,
University of Maryland, College Park, MD 20742-4111

(Dated: October 22, 2018)

We calculate the real and imaginary electron self-energy as well as the quasiparticle spectral function in doped graphene taking into account electron-electron interaction in the leading order dynamically screened Coulomb coupling. Our theory provides the basis for calculating *all* one-electron properties of extrinsic graphene. Comparison with existing ARPES measurements shows broad qualitative agreement between theory and experiment. We also calculate the renormalized graphene momentum distribution function, finding a typical Fermi liquid discontinuity at k_F . We also provide a critical discussion of the relevant many body approximations (e.g. RPA) for graphene.

PACS numbers: 81.05.Uw; 71.10.-w; 71.18.+y; 73.63.Bd

The great deal of current activity [1] in two dimensional (2D) graphene arises from its possible technological significance as a new 2D electronic material where carrier density can be controlled by an external gate voltage and from its fundamental significance as a novel 2D zero band gap semiconductor system with chiral linear Dirac-like electron-hole band energy dispersion. In particular, the chiral linear energy dispersion with the conduction and the valence band crossing at the “Dirac point” has led naturally to the interesting analogy with QED whereas the gate-induced tunability of graphene carrier density brings up the tantalizing analogy with Si MOSFETs. An important question in this context is the extent to which the Coulomb interaction between carriers will modify or renormalize the chiral linear electron-hole band dispersion in graphene.

In this Letter we theoretically consider carrier interaction effects in *extrinsic* graphene by calculating the many-body self-energy, the quasiparticle spectral function, and the renormalized momentum distribution function of graphene in the presence of free carriers (i.e. for doped or gated graphene where carriers fill the 2D band upto a Fermi level E_F). Our results show that although the quantitative renormalization effects of interactions on the graphene single-particle properties are substantial, extrinsic graphene remains an effective 2D Fermi liquid “metal”, qualitatively preserving its non-interacting chiral linear band dispersion even in the presence of mutual Coulomb interaction.

The quasiparticle spectral function, $A(\mathbf{k}, \omega)$, is a central quantity in the many-body physics of interacting systems with $A(\mathbf{k}, \omega) \equiv -2\text{Im}G(\mathbf{k}, \omega)$ where $G(\mathbf{k}, \omega)$ is the single particle (retarded) Green function for momentum \mathbf{k} and energy ω (we use $\hbar = 1$ throughout this paper). For the non-interacting bare system we immediately get $A_0(\mathbf{k}, \omega) = 2\pi\delta(\omega - \varepsilon_{s\mathbf{k}} + E_F)$ where $\varepsilon_{s\mathbf{k}} = s\gamma k$ with $k \equiv |\mathbf{k}|$ is the bare graphene linear band dispersion with $s = \pm 1$ denoting the conduction (+1) and the valence (-1) band, and $\gamma \approx 10^6$ cm/s is the band velocity. We will assume that the system is n-doped with electrons

filling the graphene conduction band upto a free carrier density (n) dependent chemical potential or Fermi level given by $E_F = \gamma k_F$, where the Fermi momentum $k_F = (\pi n)^{1/2}$. We have taken into account the spin and the valley degeneracy of graphene in obtaining the Fermi momentum. The noninteracting spectral function $A_0(\mathbf{k}, \omega)$ being a delta function signifies that the band electron at momentum \mathbf{k} has *all* its spectral weight precisely at the energy $\varepsilon_{\mathbf{k}} = \gamma k$, i.e. the noninteracting particle exists *entirely* at the energy γk for a given momentum \mathbf{k} . In the presence of interaction effects, the many-body self-energy function $\Sigma(\mathbf{k}, \omega)$ modifies the single-particle Green function: $G^{-1}(\mathbf{k}, \omega) = G_0^{-1}(\mathbf{k}, \omega) - \Sigma(\mathbf{k}, \omega)$, and the corresponding interacting or renormalized spectral function is given by

$$A(\mathbf{k}, \omega) \equiv \frac{2\text{Im}\Sigma(\mathbf{k}, \omega)}{[\omega - \xi_{\mathbf{k}} - \text{Re}\Sigma(\mathbf{k}, \omega)]^2 + [\text{Im}\Sigma(\mathbf{k}, \omega)]^2} \quad (1)$$

where $\Sigma(\mathbf{k}, \omega) = \text{Re}\Sigma(\mathbf{k}, \omega) + i\text{Im}\Sigma(\mathbf{k}, \omega)$ is complex, and $\xi_{s\mathbf{k}} \equiv \varepsilon_{s\mathbf{k}} - E_F$. In general, $A(\mathbf{k}, \omega)$ could be a complicated function of \mathbf{k} and ω , and there is no guarantee that it will have a delta function peak defining a quasiparticle. We note that $\int \frac{d\omega}{2\pi} A(\mathbf{k}, \omega) = 1$ is a sum rule, guaranteeing that the electron at momentum \mathbf{k} exists in the whole energy space, but it may exist completely incoherently spread out over the whole ω -space without any coherent structure (i.e. a delta function at $k = k_F$), indicating a complete failure of the Fermi liquid picture. Thus, the Fermi liquid theory applies *only when* the renormalized spectral function $A(k = k_F, \omega)$ at the Fermi momentum has a delta function peak, i.e. $A(k_F, \omega)$ can be written as $A(k_F, \omega) = 2\pi Z\delta(\omega - \xi_{\mathbf{k}}^*) + A_{\text{in}}(\omega)$, where Z is the so-called “renormalization factor”, $\xi_{\mathbf{k}}^*$ denotes the renormalized quasiparticle energy (measured from the chemical potential), and A_{in} is the incoherent background spectral function. If $A(k_F, \omega)$ does *not* have any delta function peak at all, then the system is a non-Fermi liquid.

In Fig. 1 we show our calculated interacting quasiparticle spectral function for extrinsic graphene at a fixed carrier density $n = 10^{12}$ cm $^{-2}$. The calculations are car-

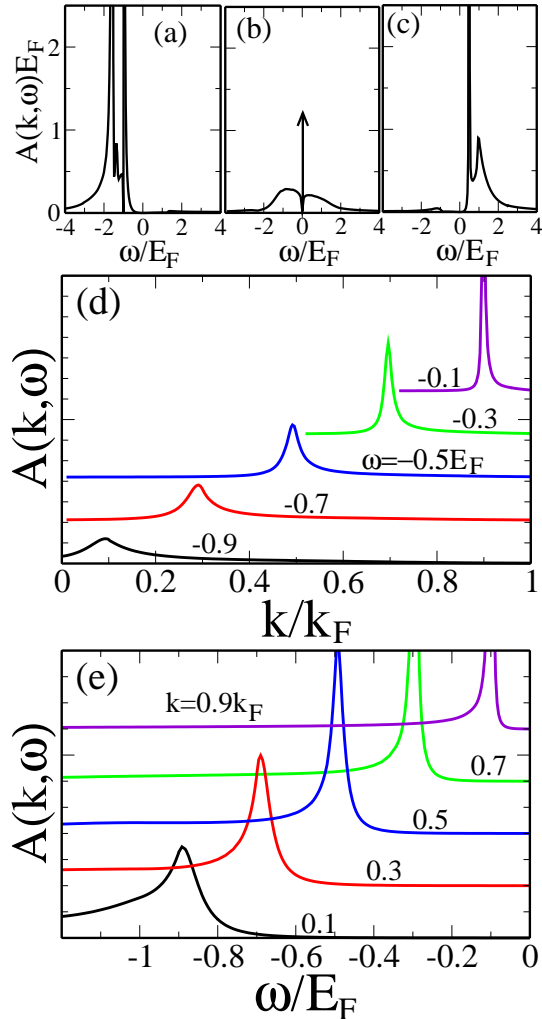


FIG. 1: Calculated graphene spectral function for different wave vectors (a) $k = 0$, (b) $k = k_F$, (c) $k = 1.5k_F$ without any disorder effects. (d) Spectral function as a function of wave vector for different energies (MDC) and (e) as a function of energy for different wave vectors (EDC). In (d) and (e) we include an impurity scattering rate of $0.5E_F$ as explained in Fig. 3(b). We only show the spectral features above the Dirac point. Here all energies are measured from the Fermi level, and the Dirac point is at $\omega = -E_F$.

ried out at $T = 0$, but thermal effects are unimportant here since $T/T_F \ll 1$ even at room temperatures. The following salient features of graphene quasiparticle spectral function are notable in Fig.1: (1) There is a well-defined delta-function quasiparticle peak at k_F with a rather substantial spectral weight of $Z \approx 0.85$, indicating that 15% of the bare spectral weight goes into incoherent background. (2) The quasiparticle spectral function for $k \neq k_F$ shows, in general, broadened peak structures indicating damped quasiparticles. (3) The generic broadened double-peak structure at $k \neq k_F$ indicates that away from the Fermi surface, the renormalized graphene spec-

tra would have two distinct energies — the second peak, which has been well-studied in the literature in both 2D [2] and 3D [3] interacting electron systems, is often referred to as the “plasmaron” peak, indicating a coupled electron-plasmon composite excitation. (4) All spectral functions for $k \neq k_F$ have finite width corresponding to quasiparticle damping defined by the imaginary part of the many-body self-energy, $\text{Im}\Sigma(k, \omega)$. Note that in Figs. 1(d) and (e) disorder contributes to combining the double peak structure into a very broadened single peak.

Since Fig. 1 giving the interacting graphene quasiparticle spectral function is the central result being presented in this paper, we first discuss the importance and the implications of our calculated spectral function before describing the details of our theory and other results. First, extrinsic (i.e. gated or doped) graphene is a Fermi liquid with a well-defined undamped quasiparticle at k_F . Thus, the chiral Dirac-like linear dispersion of graphene band structure does not lead to any anomalous non-Fermi liquid behavior. Second, extrinsic graphene has well-defined, but damped, quasiparticle peaks for all momenta. One direct experimental probe of the quasiparticle spectral function is the tunneling spectroscopy, which has been studied extensively in GaAs-based 2D systems [4], but has not yet been studied in graphene. The measurement that comes closest to studying $A(\mathbf{k}, \omega)$ in graphene is the angle-resolved-photo-emission spectroscopy (ARPES) [5, 6]. Unfortunately, there are problems in directly comparing our theoretical spectral function of Fig. 1 with the experimental ARPES results. One problem is that electron-phonon interaction induced many-body renormalization [7] and disorder also contribute to the graphene spectral function. In Figs. 1(d) and (e), we show the theoretical results corresponding to the experimental ARPES spectra — in particular, Figs. 1(d) and 1(e) respectively correspond to the so called MDC (momentum distribution curves) and EDC (energy distribution curves) of ARPES data. Since the actual theoretical spectral function, Fig. 1, has very strong momentum (k) and energy (ω) dependence, a direct comparison with ARPES data will necessarily involve detailed instrumental issues involving resolution, the (k, ω) regime of averaging, and instrumental errors which are all well beyond the scope of the current theoretical work. A very cursory comparison between our results and the experimental ARPES data [5, 6] show reasonable qualitative agreement, but short of large-scale data-fitting, one cannot make definitive quantitative statements. One important point to note here is that the plasmaron structure (i.e. the additional peak) does not really show up in the MDC and EDC spectra since they carry small spectral weight compared with the main quasiparticle peak, particularly in the energy regime near E_F as observed experimentally [5].

We now describe the theory leading to our calculation of the interacting quasiparticle spectral function de-

picted in Fig. 1. The self-energy, $\Sigma(\mathbf{k}, \omega)$, defining the spectral function through Eq. (1) is given, in the leading order dynamically screened Coulomb interaction approximation[3]

$$\Sigma_s(\mathbf{k}, i\nu_n) = -k_B T \sum_{s'} \sum_{\mathbf{q}, i\nu_n} G_{0,s'}(\mathbf{k} + \mathbf{q}, i\nu_n + i\nu_n) \times \frac{V_c(\mathbf{q})}{\epsilon(q, i\nu_n)} F_{ss'}(\mathbf{k}, \mathbf{k} + \mathbf{q}), \quad (2)$$

where $V_c(q) = 2\pi e^2/\kappa q$ is the 2D Coulomb interaction with the background lattice dielectric constant κ and $F_{ss'}(\mathbf{k}, \mathbf{k}') = (1 + ss' \cos \theta_{\mathbf{k}\mathbf{k}'})/2$ is a sublattice overlap matrix element arising from graphene band structure, and $\epsilon(q, \omega) = 1 + V_c(q)\Pi(q, \omega)$ is the dynamical RPA dielectric function for graphene with the irreducible electron-hole polarizability $\Pi(q, \omega)$, which has recently been calculated [8]. We note that the irreducible self-energy approximation used in our theory corresponds to keeping the Coulomb interaction and the infinite series of electron-hole polarizability bubble diagrams in the self-energy calculation.

An important technical point in the calculation of the self-energy is that, in general, two distinct types of field-theoretical divergence may appear in the theory: infrared (small momentum) and ultraviolet (large momentum). The infrared divergence arises from the $1/q$ long-range ($q \rightarrow 0$) divergence of the Coulomb interaction, and is regularized by our RPA theory through screening, i.e. the fact that $V_c(q)/\epsilon(q, \omega)$ does not have a $q \rightarrow 0$ infrared divergence. While the infrared self-energy divergence, which is regularized by RPA screening, is generic to all problems involving long-range Coulomb interaction, the ultraviolet divergence, which arises from the peculiar graphene band dispersion, is specific to graphene in the sense that it does not occur in the corresponding parabolic band 2D (or 3D) system [2, 3]. The ultraviolet divergence in the graphene self-energy is fixed by realizing that the linear Dirac dispersion of graphene only applies upto momenta of the order of inverse lattice constant, and therefore all momentum integrals should have an upper cut off $k_c \sim 1/a$, where a is the graphene lattice constant. We emphasize that there is nothing *ad hoc* or mysterious about this ultraviolet regularization since the band dispersion in graphene would deviate strongly from linearity for $k \geq k_c$. We also note that the infrared divergence associated with the $q \rightarrow 0$ singularity of the long-range Coulomb interaction and ultraviolet divergence associated with the $q > k_c \sim a^{-1}$ lattice wave vector scales have completely different origins, and while RPA screening fixes the infra-red divergence, the momentum cut-off fixes the ultraviolet divergence. Both infra-red and ultra-violet regularizations are important for graphene in contrast to 2D (or 3D) parabolic dispersion interacting electron systems where only the infra-red divergence is germane.

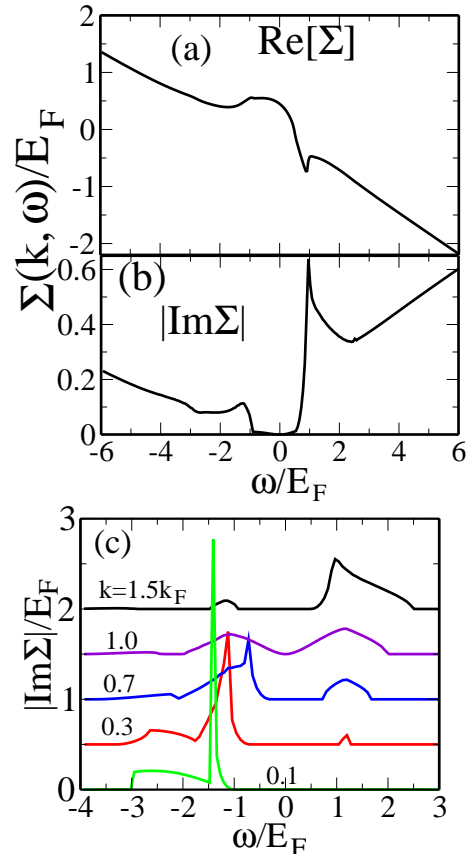


FIG. 2: Calculated graphene self energy for $k = 1.5k_F$ as a function of energy, (a) $\text{Re}\Sigma$ and (b) $|\text{Im}\Sigma|$ of correlation part. (c) Plasmon contribution to the imaginary part of self energy for several wave vectors. The Dirac point is at $\omega = -E_F$.

In Fig. 2 we show our calculated graphene self-energy for $n = 10^{12} \text{ cm}^{-2}$ at $k = 1.5k_F$. We note that the peak in $\text{Im}\Sigma$ correlates with the dip in the $\text{Re}\Sigma$, and most of the spectral weight resides near dip of $\text{Re}\Sigma$ (or equivalently, at the peak of $\text{Im}\Sigma$). We emphasize that, as is apparent from the detailed spectral function in Fig. 1, the various structures in the self-energy lead to specific features in $A(k, \omega)$ — in particular, $\text{Re}\Sigma$ and $\text{Im}\Sigma$ control respectively the energy renormalization and the broadening (or damping) of the quasiparticle. An important issue in this context is the precise contribution of the collective plasmon mode to $\text{Im}\Sigma$, which we have evaluated explicitly as shown in Fig. 2(c). Only far away from the Fermi surface the plasmon contributions are strong, giving rise to the strong plasmaron peak in the spectral function.

In Fig. 3 we show our calculated renormalized quasiparticle momentum distribution function $n(k) = \int_{-\infty}^{E_F} \frac{d\omega}{2\pi} A(k, \omega)$ for extrinsic graphene and disorder effects on the spectral function. The effect of electron-electron interaction on $n(k)$ is rather obvious in Fig. 3(a). We note that the interacting momentum distribution func-

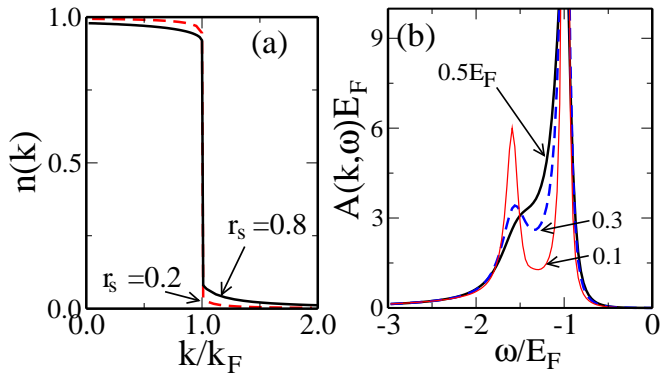


FIG. 3: (a) Renormalized momentum distribution function as a function of momentum for $r_s = 0.8$ (solid line) and 0.2 (dashed line). (b) Disorder effects on the $k = 0$ spectral function for different impurity scattering rates of 0.1, 0.3, $0.5E_F$.

tion has a discontinuity of relative size Z at $k = k_F$, clearly establishing the Fermi liquid behavior of extrinsic (i.e. doped or gated) graphene. The discontinuity increases as r_s decreases. We note here that the corresponding intrinsic (or undoped) graphene does not have a discontinuity in the distribution function since it is a marginal Fermi liquid [9].

Impurity effects are usually introduced diagrammatically into the RPA screening by including ladder impurity diagrams into the electron-hole bubble. We use a particle-conserving expression[10], which captures the essential physics of impurity scattering effects on the electron polarizability Π . We find that disorder strongly suppresses plasmon peak, but not the quasiparticle peak. Thus the double peak structure in the spectral function becomes a very broadened single peak. In the strongly disordered experimental graphene samples therefore we only have a broadened quasiparticle peak.

We now comment on the experimental implications, the theoretical approximations, and the connections to earlier work. As mentioned before, the graphene ARPES measurements have information on the electron spectral function, which are, however, complicated by the presence of additional interaction effects such as electron-impurity (i.e. disorder) and electron-phonon interactions. If these two interaction effects can be subtracted out (e.g. \sim the 200 meV structure [5] presumably arising from phonons in the experimental data), then ARPES measurements could indeed be compared with our calculated spectral function shown in Fig.1. We note that, in agreement with the ARPES data, the quasiparticle spectral peak becomes wider due to plasmon contribution as the energy approaches to the Dirac point ($\omega = -E_F$). Including disorder effects, indeed there is good agreement between theory and experiment.

Our theory is based on the leading-order expansion of the electron self-energy using the dynamically

screened Coulomb interaction (the so-called infinite bubble diagram expansion with each bubble being the non-interacting electron-hole polarizability [8]), which we believe to be a quantitatively accurate approximation for extrinsic graphene (i.e. at any finite carrier density) by virtue of graphene having a reasonably small (and density independent) dimensionless interaction parameter $r_s = e^2/\kappa\gamma \sim 0.8$ (0.4) for graphene on SiO_2 (SiC) substrate. In fact, the same self-energy approximation, often referred to in the literature as “RPA” or “GW” approximation, is known to work well in 3D alkali metals where $r_s \sim 3 - 6$ [3] and in 2D semiconductor system [2, 4] where $r_s \sim 1 - 10$. For extrinsic graphene only the terms having bubble diagrams (or RPA type diagrams) in self-energy have the infra-red divergence. All other vertex corrections (i.e. non-RPA type diagrams) have finite values. Thus, most contributions (for $r_s < 1$) come from RPA type diagrams. Since we can control the ultra-violet divergence by introducing a physical energy cut-off, our RPA approach is quantitatively accurate for extrinsic graphene. However, for intrinsic graphene, there is no infra-red divergence in RPA type diagrams, only the ultra-violet divergence. Since all diagrams then contribute to the self-energy, the perturbative expansion does not converge for intrinsic graphene. Therefore, RPA is not a meaningful approximation for intrinsic graphene, and indeed it predicts a non-Fermi liquid behavior [9].

In discussing connection between our work and earlier work, we mention that, although there has been a great deal of recent theoretical work on interaction effects in graphene, much of it has focused on intrinsic graphene [11], and most of the work on extrinsic graphene has focused on thermodynamic properties [12]. A recent calculation of the quasiparticle spectral function in graphene due to electron-phonon interaction has appeared [7] in the literature, and within the weak-coupling theory (i.e. both electron-electron and electron-phonon interactions being weak), the total spectral function should be a sum of these two spectral functions. We do note that our calculated spectral function and self-energy in extrinsic graphene is qualitatively rather similar to that in ordinary parabolic band 2D carrier systems [2], thus pointing to the fact that, in spite of its chiral Dirac-like band dispersion, doped graphene in the presence of free carriers is qualitatively similar to doped 2D semiconductor systems.

In summary, we have calculated the electron spectral function in 2D doped (i.e. extrinsic) graphene, finding our theory to be in good qualitative agreement with the available experimental data. Our theory convincingly demonstrates the Fermi liquid nature of doped graphene.

This work is supported by U.S. ONR and LPS-NSA.

-
- [1] S. Das Sarma, A. K. Geim, P. Kim, and A. H. MacDonald, eds., *Exploring Graphene: Recent Research Advances, A Special Issue of Solid State Communications*, vol. 143 (Elsevier, 2007); references therein.
- [2] R. Jalabert and S. Das Sarma, Phys. Rev. B **40**, 9723 (1989).
- [3] L. Hedin and S. Lundqvist, in *Solid State Physics*, edited by H. Ehrenreich *et al.* (Academic, New York, 1969), Vol. 23.
- [4] S. Q. Murphy *et al.*, Phys. Rev. B **52**, 14825 (1995); J.P. Eisenstein *et al.*, Solid State Commun. **143**, 365 (2007).
- [5] A. Bostwick *et al.*, Nature Phys. **3**, 36 (2007).
- [6] S. Y. Zhou *et al.*, Nature Phys. **2**, 595 (2006).
- [7] M. Calandra and F. Mauri, arXiv:0707.1467; C. H. Park *et al.*, arXiv:0707.1666; W. K. Tse and S. Das Sarma, arXiv:0707.3651.
- [8] E. H. Hwang and S. Das Sarma, Phys. Rev. B **75**, 205418 (2007).
- [9] S. Das Sarma *et al.*, Phys. Rev. B **75**, 121406 (2007).
- [10] D. Mermin, Phys. Rev. B **1**, 2362 (1970).
- [11] J. González *et al.* Phys. Rev. Lett. **77**, 3589 (1996); D. V. Khveshchenko, Phys. Rev. B **74**, 161402(R) (2006).
- [12] E. H. Hwang *et al.*, cond-mat/0703499; cond-mat/0612345; Y. Barlas *et al.*, Phys. Rev. Lett. **98**, 236601(2007); M. Polini *et al.*, Solid. State. Commun. **143**, 58 (2007).